Progress In Electromagnetics Research M, Vol. 102, 81–89, 2021

Asymmetric Impedance Vibrator for Multi-Band Communication Systems

Mikhail V. Nesterenko*, Victor A. Katrich, Sergey L. Berdnik, Oleksandr M. Dumin, and Yevhenii O. Antonenko

Abstract—A numeric-analytical solution of a problem concerning an impedance vibrator with local asymmetric excitation is derived in the thin-wire approximation. Solution correctness is confirmed by satisfactory agreement of numerical and experimental results from well-known literary sources. Based on the optimization modeling, the design of the impedance antenna characterized by three resonant frequencies intended for mobile communications operating in GSM 900, GSM 1800, and WiMAX ranges is developed. The analysis of basic electrodynamic characteristics of the vibrator antenna has proved the possibility of practical applications of this antenna for phones, portable radio stations, electronic gadgets, and base stations.

1. INTRODUCTION

The modern world and its further development cannot be imagined without mobile communication technology. One of the functional elements of cell phones is a single- or multi-element antenna. A large number of publications have been devoted to designing the antennas for mobile devices (see, for example, [1–3] and references therein). The development of mobile communication systems requires that mobile phones operate in several frequency ranges, for example, in the GSM 900 ($880 \div 960$ MHz), GSM 1800 ($1710 \div 1880$ MHz) ranges adopted in Europe and Asia, or in GSM 850 and GSM 1900 ranges adopted in North America. In the early stages of cellular communication development, the following external antennas: rectilinear perfectly con-ducting vibrators [4, 5], capacitive type impedance monopoles [6], inductive spiral impedance antennas [7, 8], cone-shaped antennas [9], and combinations of monopoles and spirals [10–12] were mainly used. In all known cases, only antennas with symmetric excitation have been developed. Of course, the multi-frequency antenna operation implemented by expanding operating band can cause a significant weakening of its noise-immunity properties. Therefore, designers traditionally resort to combining several antennas operating at different frequencies [10–16]. This approach complicates the design of an antenna module and is an obstacle to its miniaturization.

Among the recent publications devoted to multi-band printed antennas integrated in the phone case, references [17–23] should be noted, where the antenna characteristics were obtained by using commercial programs such as HFSS, CST Microwave Studio, and others. Calculating and optimizing the antenna characteristics by using this approach require the enumeration of a large number of options, hence, large amount of computer time and resources.

The use of vibrators with an asymmetric excitation point to create multi-band antennas has been proposed by many researchers [13, 15, 24–26]. However, in the listed publications, only perfectly conducting vibrators were considered, which did not allow tuning the antenna to specified frequencies. As an alternative, a vibrator impedance antenna with asymmetric excitation integrated in the phone

Received 12 March 2021, Accepted 9 April 2021, Scheduled 14 April 2021

* Corresponding author: Mikhail V. Nesterenko (mikhail.v.nesterenko@gmail.com).

The authors are with the Department of Radiophysics, Biomedical Electronics and Computer Systems, V. N. Karazin Kharkiv National University, 4, Svobody Sq., Kharkiv 61022, Ukraine.

case can be offered. In this case, the frequency response of the antenna may have several pronounced resonances, preventing from receiving signals beyond the resonance bands. The analysis of such antennas could not be found in literature, which makes their study extremely relevant from a practical point of view.

This paper is aimed at studying a multi-band antenna for cell phones and mobile communication systems based on the asymmetric vibrator with inductive surface impedance. The antenna can operate in the GSM 900, GSM 1800, and WiMAX ($3.4 \div 3.6$ GHz) ranges. The antenna characteristics will be modelled by using the numerical-analytical method, known as generalized method of induced electromotive forces (EMF), proposed by the authors earlier in [27, 28].

2. PROBLEM FORMULATION AND SOLUTION

For the convenience of readers, we briefly present the solution to the problem for a vibrator with a distributed surface impedance with asymmetric excitation. The integral equation relative to the vibrator current will be solved by the asymptotic averaging method [29], based on the results obtained in the frameworks of classical thin-wire approximation, in which only the longitudinal current component along the vibrator axis was taken into account, while the transverse component, including that in the neighborhood of ends of the vibrator arm and on the ends of real radiating constructions, was neglected.

Consider the vibrator, represented by a rectilinear circular cylinder, asymmetrically exited by extraneous sources. The vibrator radius and length, r and $2L$, satisfy the thin-wire approximation $(r/2L) \ll 1$, $(r/\lambda_1) \ll 1$, where λ_1 is the wavelength in the medium. The excitation fields of extraneous sources E_{0s} and intrinsic linear vibrator impedance z_i, can be divided into symmetric and antisymmetric components relative to the vibrator geometrical center. These components marked by the indices "s" and "a" are presented as $E_{0s}(s) = E^s_{0s}(s) + E^a_{0s}(s)$ and $z_i(s) = z^s_i(s) + z^a_i(s)$. Quite naturally, the vibrator currents can also have two components $J(s) = J^s(s) + J^a(s)$. The initial equation relative to the vibrator current obtained by using the boundary condition $J(\pm L) = 0$ has the following form

$$\left(\frac{d^2}{ds^2} + k_1^2\right) \int\limits_{-L}^{L} \left[J^s(s') + J^a(s')\right] G_s(s, s')\, ds' = -i\omega\varepsilon_1 \left\{\left[E^s_{0s}(s) + E^a_{0s}(s)\right] - \left[z^s_i(s) + z^a_i(s)\right]\left[J^s(s) + J^a(s)\right]\right\}, \quad (1)$$

where $E^{s,a}_{0s}(s)$ are the projections of extraneous source fields on the vibrator axis; $G_s(s, s') = \frac{e^{-ik_1\sqrt{(s-s')^2+r^2}}}{\sqrt{(s-s')^2+r^2}}$; s and s' are the local coordinates related to the vibrator axis and surface; $k_1 = k_1' - ik_1'' = k\sqrt{\varepsilon_1\mu_1}$, $k = 2\pi/\lambda$, where λ is the wavelength in free space; ε_1 and μ_1 are the permittivity and permeability of the medium. The monochromatic fields and currents depend on time t as $e^{i\omega t}$ ($\omega = 2\pi f$ is the circular frequency, and f is the frequency, measured in Hz).

Equation (1) can be represented by the system of two coupled integral equations, relative to the unknown currents $J^s(s)$ and $J^a(s)$

$$\begin{cases} \left(\dfrac{d^2}{ds^2} + k_1^2\right) \displaystyle\int\limits_{-L}^{L} J^s(s') G_s(s, s')\, ds' = -i\omega\varepsilon_1 \{E^s_{0s}(s) - [z^s_i(s) J^s(s) + z^a_i(s) J^a(s)]\}, \\ \left(\dfrac{d^2}{ds^2} + k_1^2\right) \displaystyle\int\limits_{-L}^{L} J^a(s') G_s(s, s')\, ds' = -i\omega\varepsilon_1 \{E^a_{0s}(s) - [z^s_i(s) J^a(s) + z^a_i(s) J^s(s)]\}. \end{cases} \quad (2)$$

The vibrator currents can be presented as the product of the unknown complex amplitudes $J^{s,a}_n$ and weight functions $f^{s,a}_n(s')$ $(n = 0, 1)$ as

$$J^{s,a}(s') = J^{s,a}_0 f^{s,a}_0(s') + J^{s,a}_1 f^{s,a}_1(s'), \quad f^{s,a}_n(\pm L) = 0. \quad (3)$$

The solution of the equations system (2) can be obtained by the generalized method of induced EMF [27, 28]. To do so, let us multiply the left- and right-hand parts of Equation (2) by functions

$f_n^s(s)$ and $f_n^a(s)$, and integrate the resulting expressions over the vibrator length. Thus, the following algebraic equations system (SLAE) is obtained

$$\begin{cases} J_0^s Z_{00}^{s\Sigma} + J_1^s Z_{01}^{s\Sigma} + J_0^a \tilde{\tilde{Z}}_{00}^{sa} + J_1^a \tilde{\tilde{Z}}_{01}^{sa} = -(i\omega/2k)E_0^s, \\ J_0^s Z_{10}^{s\Sigma} + J_1^s Z_{11}^{s\Sigma} + J_0^a \tilde{\tilde{Z}}_{10}^{sa} + J_1^a \tilde{\tilde{Z}}_{11}^{sa} = -(i\omega/2k)E_1^s, \\ J_0^a Z_{00}^{a\Sigma} + J_1^a Z_{01}^{a\Sigma} + J_0^s \tilde{\tilde{Z}}_{00}^{as} + J_1^s \tilde{\tilde{Z}}_{01}^{as} = -(i\omega/2k)E_0^a, \\ J_0^a Z_{10}^{a\Sigma} + J_1^a Z_{11}^{a\Sigma} + J_0^s \tilde{\tilde{Z}}_{10}^{as} + J_1^s \tilde{\tilde{Z}}_{11}^{as} = -(i\omega/2k)E_1^a, \end{cases} \tag{4}$$

where $(m = 0, 1;\ n = 0, 1)$,

$$\begin{aligned} Z_{mn}^{s,a} &= \frac{1}{2k}\left\{ -\frac{df_m^{s,a}(s)}{ds} A_n^{s,a}(s)\Big|_{-L}^{L} + \int_{-L}^{L} \left[\frac{d^2 f_m^{s,a}(s)}{ds^2} + k_1^2 f_m^{s,a}(s)\right] A_n^{s,a}(s) ds \right\}, \\ A_n^{s,a}(s) &= \int_{-L}^{L} f_n^{s,a}(s') G_s(s, s') ds', \\ \tilde{Z}_{mn}^{s,a} &= -\frac{i\omega}{2k} \int_{-L}^{L} f_m^{s,a}(s) f_n^{s,a}(s) z_i^s(s) ds, \quad Z_{mn}^{(s,a)\Sigma} = Z_{mn}^{s,a} + \tilde{Z}_{mn}^{s,a}, \\ \tilde{\tilde{Z}}_{mn}^{\begin{Bmatrix} sa \\ as \end{Bmatrix}} &= -\frac{i\omega}{2k} \int_{-L}^{L} f_m^{\begin{Bmatrix} s \\ a \end{Bmatrix}}(s) f_n^{\begin{Bmatrix} a \\ s \end{Bmatrix}}(s) z_i^a(s) ds, \quad E_m^{s,a} = \int_{-L}^{L} f_m^{s,a}(s) E_{0s}^{s,a}(s) ds. \end{aligned} \tag{5}$$

If the symmetric and asymmetric parts of the vibrator impedance are $z_i^s(s) = \text{const}$ and $z_i^a(s) = 0$, the SLAE in Eq. (4) can be divided into two independent equation systems relative to the unknown currents J_n^s and J_n^a

$$\begin{cases} J_0^s Z_{00}^{s\Sigma} + J_1^s Z_{01}^{s\Sigma} = -(i\omega/2k)E_0^s, \\ J_0^s Z_{10}^{s\Sigma} + J_1^s Z_{11}^{s\Sigma} = -(i\omega/2k)E_1^s, \end{cases} \quad \begin{cases} J_0^a Z_{00}^{a\Sigma} + J_1^a Z_{01}^{a\Sigma} = -(i\omega/2k)E_0^a, \\ J_0^a Z_{10}^{a\Sigma} + J_1^a Z_{11}^{a\Sigma} = -(i\omega/2k)E_1^a, \end{cases} \tag{6}$$

and the vibrator current can be written as $J(s) = J^s(s) + J^a(s)$, where

$$J^{s,a}(s) = -\frac{i\omega\varepsilon_1}{2k}\left[\frac{E_0^{s,a} Z_{11}^{(s,a)\Sigma} - E_1^{s,a} Z_{01}^{(s,a)\Sigma}}{Z_{00}^{(s,a)\Sigma} Z_{11}^{(s,a)\Sigma} - Z_{10}^{(s,a)\Sigma} Z_{01}^{(s,a)\Sigma}} f_0^{s,a}(s) + \frac{E_1^{s,a} Z_{00}^{(s,a)\Sigma} - E_0^{s,a} Z_{10}^{(s,a)\Sigma}}{Z_{00}^{(s,a)\Sigma} Z_{11}^{(s,a)\Sigma} - Z_{10}^{(s,a)\Sigma} Z_{01}^{(s,a)\Sigma}} f_1^{s,a}(s) \right]. \tag{7}$$

3. IMPEDANCE VIBRATOR EXCITED IN AN ARBITRARY POINT

Let the vibrator with the impedance $(z_i^s(s) = \text{const},\ z_i^a(s) = 0)$ be excited in the point $s = -s_\delta$ by the voltage generator with amplitude V_0, as shown in Fig. 1. Then

$$\begin{aligned} E_{0s}(s) &= V_0 \delta(s + s_\delta) = E_{0s}^s(s) + E_{0s}^a(s), \\ E_{0s}^s(s) &= \frac{V_0}{2}\left[\delta(s + s_\delta) + \delta(s - s_\delta)\right], \\ E_{0s}^a(s) &= \frac{V_0}{2}\left[\delta(s + s_\delta) - \delta(s - s_\delta)\right], \end{aligned} \tag{8}$$

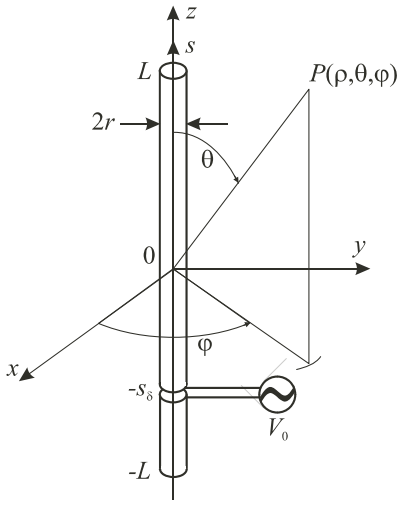

Figure 1. The vibrator geometry and accepted designations.

where δ is the Dirac delta function. In this case, the vibrator current defined by Eq. (7) can be written as $J(s) = J^s(s) + J^a(s)$, where

$$J^{s,a}(s) = -\frac{i\omega\varepsilon_1}{2k}V_0\left[\frac{\tilde{E}_0^{s,a}Z_{11}^{(s,a)\Sigma} - \tilde{E}_1^{s,a}Z_{01}^{(s,a)\Sigma}}{Z_{00}^{(s,a)\Sigma}Z_{11}^{(s,a)\Sigma} - Z_{10}^{(s,a)\Sigma}Z_{01}^{(s,a)\Sigma}}f_0^{s,a}(s) + \frac{\tilde{E}_1^{s,a}Z_{00}^{(s,a)\Sigma} - \tilde{E}_0^{s,a}Z_{10}^{(s,a)\Sigma}}{Z_{00}^{(s,a)\Sigma}Z_{11}^{(s,a)\Sigma} - Z_{10}^{(s,a)\Sigma}Z_{01}^{(s,a)\Sigma}}f_1^{s,a}(s)\right]. \tag{9}$$

Let us choose the functions $f_0^{s,a}(s)$ obtained after substituting the expressions (8) into the general solution of the equation for the current by the averaging method in the form:

$$\begin{aligned} f_0^s(s) &= \cos\tilde{k}_1 s_\delta \sin\tilde{k}_1 L\cos\tilde{k}_1 s\ - (1/2)\cos\tilde{k}_1 L(\sin\tilde{k}_1|s-s_\delta| + \sin\tilde{k}_1|s+s_\delta|),\\ f_0^a(s) &= \sin\tilde{k}_1 s_\delta \cos\tilde{k}_1 L\sin\tilde{k}_1 s\ + (1/2)\sin\tilde{k}_1 L(\sin\tilde{k}_1|s-s_\delta| - \sin\tilde{k}_1|s+s_\delta|), \end{aligned} \tag{10}$$

where $\tilde{k}_1 = k_1 - \frac{i\bar{Z}_S\sqrt{\varepsilon_1/\mu_1}}{2r\ln(2L/r)}$, $\bar{Z}_S = \bar{R}_S + i\bar{X}_S = 2\pi r z_i/Z_0$ is the distributed surface impedance, normalized on the free space wave impedance, $Z_0 = 120\pi$ OHm. The current distribution function $f_1^s(s)$ is defined in [27], and the function $f_1^a(s)$ can be found as the solution of integral Equation (1), obtained for the case $z_i = 0$ [24]. These functions can be written as:

$$f_1^s(s) = \cos\tilde{k}_1 s - \cos\tilde{k}_1 L, \tag{11a}$$

$$f_1^a(s) = \sin k_1 s - (s/L)\sin k_1 L. \tag{11b}$$

The coefficients $Z_{mn}^{s,a}(m = 0,1;\ n = 0,1)$ in Equation (9) can be obtained by substituting Equations (10) and (11) into Equation (5)

$$Z_{0n}^s = \frac{\tilde{k}_1}{k}\left[\cos\tilde{k}_1 s_\delta\, A_n^s(L) - \cos\tilde{k}_1 L\, A_n^s(s_\delta)\right] + \frac{(k_1^2-\tilde{k}_1^2)}{2k}\int\limits_{-L}^{L} f_0^s(s)A_n^s(s)ds,$$

$$Z_{1n}^s = \frac{\tilde{k}_1}{k}\sin\tilde{k}_1 L\, A_n^s(L)\ - \frac{1}{2k}\left[k_1^2\cos\tilde{k}_1 L\int\limits_{-L}^{L} A_n^s(s)ds - (k_1^2-\tilde{k}_1^2)\int\limits_{-L}^{L}\cos\tilde{k}_1 s A_n^s(s)ds\right],$$

$$Z_{0n}^a = -\frac{\tilde{k}_1}{k}\left[\sin\tilde{k}_1 s_\delta\, A_n^a(L) - \sin\tilde{k}_1 L\, A_n^a(s_\delta)\right]\ + \frac{(k_1^2-\tilde{k}_1^2)}{2k}\int\limits_{-L}^{L} f_0^a(s)A_n^a(s)ds,$$

$$Z_{1n}^a = \frac{k_1}{k}\left(\frac{\sin k_1 L}{k_1 L} - \cos k_1 L\right)A_n^a(L) - \frac{k_1^2}{2kL}\sin k_1 L\int\limits_{-L}^{L} A_n^a(s)sds,$$

$$\tilde{Z}^{s,a}_{mn} = \frac{\bar{Z}_S}{ir}\int\limits_{-L}^{L} f^{s,a}_m(s) f^{s,a}_n(s) ds,$$

$$\tilde{E}^s_0 = \cos\tilde{k}_1 s_\delta \sin\tilde{k}_1 (L - |s_\delta|), \quad \tilde{E}^s_1 = \cos\tilde{k}_1 s_\delta - \cos\tilde{k}_1 L,$$
$$\tilde{E}^a_0 = -\sin\tilde{k}_1 |s_\delta| \sin\tilde{k}_1 (L - |s_\delta|), \quad \tilde{E}^a_1 = \sin k_1 s_\delta - (s_\delta/L)\sin k_1 L.$$

The input impedance $Z_{in} = R_{in} + iX_{in}$ and admittance $Y_{in} = G_{in} + iB_{in}$ can be presented as:

$$Z_{in}[\text{Ohm}] = \frac{60i/\varepsilon_1}{J^s_0 f^s_0(s_\delta) + J^s_1 f^s_1(s_\delta) + J^a_0 f^a_0(s_\delta) + J^a_1 f^a_1(s_\delta)}, \quad Y_{in}[\text{millimhos}] = \frac{10^3}{Z_{in}}. \tag{12}$$

Then, the voltage standing wave ratio ($VSWR$) in the antenna feeder with the wave impedance W is equal to:

$$VSWR = \frac{1 + |S_{11}|}{1 - |S_{11}|}, \tag{13}$$

where $S_{11} = \frac{Z_{in} - W}{Z_{in} + W}$ is the reflection coefficient in the feeder.

The comparison of the calculated and the experimental results in [27, 28] allows us to state that the approximating functions in Eqs. (10) and (11) adequately represent the real physical process if the electrical lengths of the vibrator $(2L/\lambda) \leq 1.4$. Two other approximating functions $f^s_2(s)$ and $f^a_2(s)$ valid in the range $1.4 < (2L/\lambda) \leq 2.5$ can also be substituted in Equation (3). These functions were obtained in [30] in the form

$$f^s_2(s) = \cos\frac{k_1 s}{2} - \cos\frac{k_1 L}{2}, \quad f^a_2(s) = \sin\frac{k_1 s}{2} - \sin\frac{k_1 L}{2}. \tag{14}$$

If the perfectly conducting vibrator is coated by the magnetodielectric with permittivity $\varepsilon = \varepsilon' - i\varepsilon''$ and permeability $\mu = \mu' - i\mu''$, the formula for the inductive surface impedance is $\bar{Z}_S = i\sqrt{\mu_1/\varepsilon_1} kr\mu \ln(r/r_i)$, where r and r_i are the vibrator and coating radii. This formula is valid if condition $|(k\sqrt{\varepsilon\mu}r)^2 \ln(k\sqrt{\varepsilon\mu}r_i)| \ll 1$ is satisfied [27]. If $\varepsilon_1 = \mu_1 = 1$, the formula is reduced to $\bar{Z}_S = ikrC_L$, where constant C_L is determined by the vibrator geometrical dimensions and electrical-physical parameters of the vibrator material.

The mathematical model is verified by comparing calculated and experimental data. The comparison results for the medium with material parameters $\varepsilon_1 = \mu_1 = 1$ can be found, for example, in [31 (Fig. 2), 32].

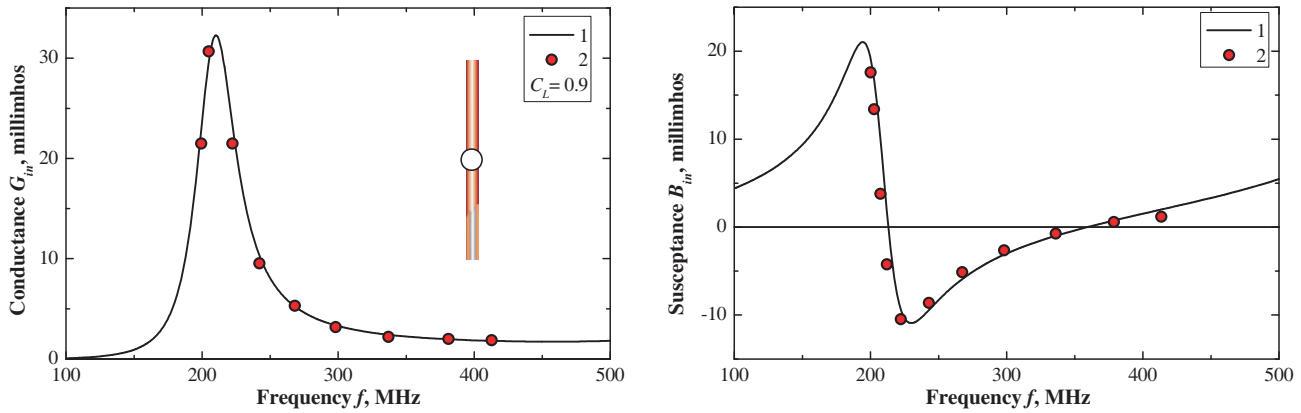

Figure 2. The input admittance of the metallic conductor of the radius $r_i = 0.5175$ cm, covered by the ferrite ($\mu = 4.7$) shell of the radius $r = 0.6$ cm versus frequency at $2L = 30.0$ cm, $s_\delta = 0.0$: 1 — calculation (the functions (10) and (11)), 2 — experimental data [31].

4. NUMERICAL RESULTS

The characteristics of vibrator antennas were calculated by the equivalent circuit method [33]. According to this approach, the antenna is put into correspondence with an equivalent distributed or lumped circuit. The circuit parameters are selected so that the input vibrator impedance could best approximate the frequency response of the antenna input impedance. This approach has not yet received a rigorous theoretical justification for different antennas, but the results obtained for thin wire antennas are in good agreement with experimental data for the antennas whose lengths are shorter than wavelength λ [33]. In general, the method allows an obvious physical interpretation of the calculation results; therefore, we will use this approach below.

In our case, the vibrator antenna with asymmetric excitation can be put into correspondence with the equivalent circuit consisting of two parallel three-element reactive double-pole circuits, coupling with one another by electromagnetic interaction over the external space. Suppose that double-pole circuit is tuned to the frequencies f_1 and f_2 ($f_1 \leq f_2$), corresponding to lengths of the vibrator arms. The frequencies f_1 and f_2 are defined as normal. According to the general theory of oscillations, the superposition of the two normal modes will also emerge in the excited vibrator due to the external coupling of the double-pole circuits. Thus, a beating at the frequency $f_\delta = f_2 - f_1$ is formed. However, energy from one circuit to another will "flow" not only at the beat frequency f_δ, but also at its higher harmonics. Thus, a hypothetical possibility for tuning the vibrator to several resonant frequencies arises. If, for example, the lengths of the vibrator arms are selected so that the normal resonant frequencies $f_1 \approx 0.9\,\text{GHz}$ and $f_2 \approx 1.8\,\text{GHz}$ belong to the GSM 900 and GSM 1800 ranges, the higher resonances will be a multiple of the beat frequency $f_\delta \approx 0.9\,\text{GHz}$. Consequently, the vibrator antenna can operate at the three-frequencies: $f_1 \approx 0.9\,\text{GHz}$, $f_2 \approx 1.8\,\text{GHz}$ and $f_3 \approx 3.5\,\text{GHz}$ from the WiMAX range.

The preliminary analysis of frequency response has allowed us to formulate a goal of the computational experiment directed for optimization of the vibrator radiator. The goal is to confirm, based on rigorous electrodynamic modeling, the possibility of tuning the impedance vibrator with asymmetric excitation at three predefined resonant frequencies. Multiparameter calculations have allowed us to define the vibrator antenna design with the required input resistance based on the perfectly conducting cylinder coated by a uniform magnetic layer ($\mu = 4.7$). The vibrator parameters are as follows: total length $2L$ =120 mm; radius is 1.37 mm, external coating radius is 2 mm; and the local coordinate of the excitation point $s_\delta = -0.395L$. That is, the lengths of the vibrator arms should be equal to 36.3 mm and 83.7 mm. The frequency plots of the reflection coefficient $|S_{11}|$ in Eq. (13) for the vibrator antenna are presented in Fig. 3, where the boundaries of standard frequency ranges of the GSM 900 (880 ÷ 960 MHz), GSM 1800 (1710 ÷ 1880 MHz), WiMAX (3400 ÷ 3600 MHz) bands are

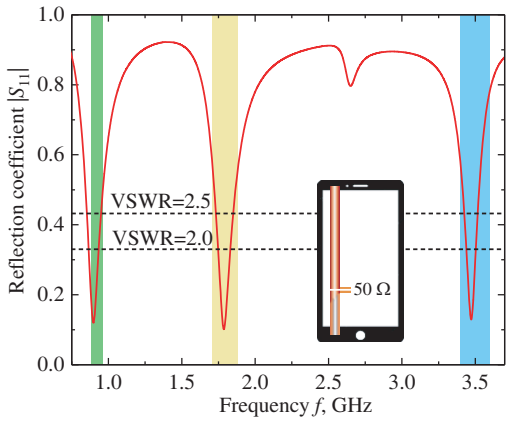

Figure 3. The reflection coefficient $|S_{11}|$ of the metallic conductor of the radius $r_i = 1.37\,\text{mm}$, covered by the ferrite ($\mu = 4.7$) shell of the radius $r = 2.0\,\text{mm}$ ($C_L = 1.776$) versus frequency at $2L = 120.0\,\text{mm}$, $s_\delta = -0.395L$.

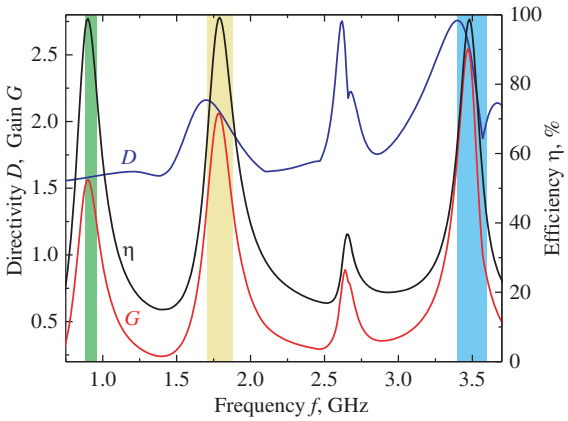

Figure 4. The directivity D, gain G, and efficiency η of the triple-band antenna.

marked by color strips. The dimensions of the proposed antenna are compared with dimensions of a typical smartphone case which are also shown in Fig. 3.

As can be seen from Fig. 3, the impedance antenna is indeed characterized by three resonant frequencies $f_1 = 0.9\,\text{GHz}$, $f_2 = 1.79\,\text{GHz}$, and $f_3 = 3.48\,\text{GHz}$ with operating bands $\{0.866, 0.935\}$, $\{1.750, 1.835\}$ and $\{3.446, 3.512\}$ GHz at the VSWR level 2.0. It should be noted that if $VSWR = 2.5$ the operating bands of the impedance antenna almost completely cover the frequency ranges of GSM 900 and GSM 1800, and 46% of the WiMAX range.

The simulation results have also confirmed that the electrodynamic characteristics of the triple-band antenna satisfy the requirements of practice. The frequency plots of the main antenna characteristic: directivity D, efficiency $\eta = 1 - |S_{11}|^2$, and gain $G = \eta D$ are presented in Fig. 4. The directivity is calculated by the formula

$$D = \frac{2}{\int\limits_0^{\pi} |F(\theta)|^2 \sin(\theta)\, d\theta}, \tag{15}$$

where the antenna radiation pattern (RP) $F(\theta)$ in the denominator of Eq. (15) is calculated by the formula $F(\theta) = \frac{\sin(\theta)}{F_{\max}} \int\limits_{-L}^{L} J(s) e^{iks\cos(\theta)} ds$, where $F_{\max}$ is the normalizing factor.

As expected, the antenna H-plane RP is uniform in the angle φ, while the E-plane RP, naturally, is multi-lobe. The normalized RPs of the impedance antenna at three resonant frequencies are shown in Fig. 5. Note that if the spatial orientation of the mobile device antenna varies randomly in time, the E-plane RP averaged over time can be considered as quasi-isotropic.

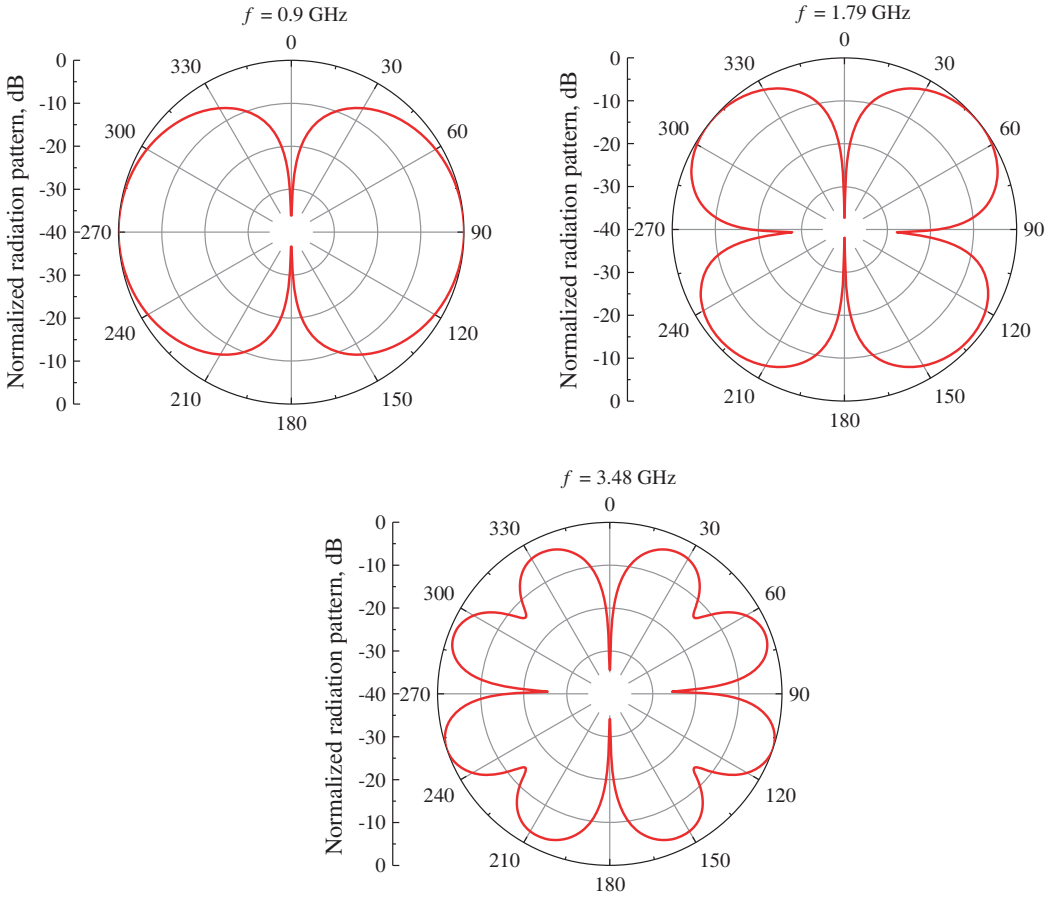

Figure 5. The RPs of the triple-band antenna.

5. CONCLUSION

The design of the electrically thin impedance vibrator antenna with asymmetric excitation operating at three frequencies, based on the results of rigors electrodynamic modeling is proposed. The operating bands of the impedance antenna, limited by the input $VSWR = 2.5$, are within the frequency ranges of GSM 900 ($880 \div 960$ MHz), GSM 1800 ($1710 \div 1880$ MHz), and WiMAX ($3.4 \div 3.6$ GHz). It is shown that the gain and efficiency of the vibrator antenna in the operating ranges are quite satisfactory. The characteristic property of the antenna is the possibility of resonant tuning to the selected frequencies, which does not decrease the noise-resistant properties as compared with broadband antennas. The obtained results allow us to conclude that the vibrator antenna can be used in phones, portable radio stations, electronic gadgets, and base stations operating in three standard frequency ranges. It should also be noted that in order to eliminate the influence of the internal structures of the used communication devices, this antenna should be placed over a rectangular perfectly conducting screen of finite dimensions or dihedral corner reflector (in this case, the effect on the human body is significantly reduced) [34–36]. These publications also show that the presence of a screen practically does not affect the resonant characteristics of an impedance vibrator antenna, but at the same time increases its efficiency.

REFERENCES

1. Chen, Z. N., *Antennas for Portable Devices*, Wiley, Chichester, England, 2007.
2. Fujimoto, K. and J. R. James, *Mobile Antenna Systems Handbook*, Artech House, London, England, 2008.
3. Zhang, Z., *Antenna Design for Mobile Devices*, Wiley, London, England, 2017.
4. Geissler, M. and D. Heberling, "An optimized antenna for mobile phones," *Proceedings IEEE AP-S International Symposium*, Vol. 1, 118–121, 1998.
5. Liu, D., "A dual-band antenna for cellular applications," *Proceedings IEEE AP-S International Symposium*, Session 28, 786–789, 1998.
6. Nesterenko, M. V. and V. A. Katrch, "Thin vibrators with arbitrary surface impedance as a handset antennas," *Proceedings 5th European Personal Mobile Communications Conference*, 16–20, 2003.
7. Zhou, G., "A non-uniform pitch dual band helix antenna," *Proceedings IEEE AP-S International Symposium*, Vol. 1, 274–277, 2000.
8. Egorov, I. and Z. Ying, "A non-uniform helical antenna for dual-band cellular phones," *Proceedings IEEE AP-S International Symposium*, Vol. 2, 652–655, 2000.
9. Wong, K.-L. and S.-L. Chien, "Wide-band cylindrical monopole antenna for mobile phone," *IEEE Trans. Antennas Propag.*, Vol. 53, No. 8, 2756–2758, 2005.
10. Zhou, G. and B. Yildirim, "A multi-band fixed cellular phone antenna," *Proceedings IEEE AP-S International Symposium*, Vol. 1, 112–115, 1999.
11. Odachi, N., S. Sekine, H. Shoki, and Y. Suzuki, "A rod antenna with a meander element for hand-held phone," *Proceedings IEEE AP-S International Symposium*, Vol. 3, 1682–1685, 2000.
12. Tung, H.-C., C.-Y. Fang, and K.-L. Wong, "Dual-band inverted-L monopole antenna for GSM/DCS mobile phone," *Proceedings IEEE AP-S International Symposium*, Vol. 3, 30–33, 2002.
13. Song, C., Y. Huang, J. Zhou, P. Carter, S. Yuan, Q. Xu, and Z. Fei, "Matching network elimination in broadband rectennas for high-efficiency wireless power transfer and energy harvesting," *IEEE Trans. Industrial Electronics*, Vol. 64, 3950–3961, 2017.
14. Paramayudha, K., S. J. Chen, T. Kaufmann, W. Withayachumnankul, and C. Fumeaux, "Triple-band reconfigurable low-profile monopolar antenna with independent tenability," *IEEE Open J. Antennas Propag.*, Vol. 1, 47–56, 2020.
15. Hu, W., T. Feng, S. Gao, L. Wen, Q. Luo, P. Fei, Y. Liu, and X. Yang, "Wideband circularly polarized antenna using single-arm coupled asymmetric dipoles," *IEEE Trans. Antennas Propag.*, Vol. 68, 5104–5113, 2020.
16. Luo, Y. and Y. Liu, "Nona-band antenna with small nonground portion for full-view display mobile phones," *IEEE Trans. Antennas Propag.*, Vol. 68, 7624–7629, 2020.

17. Wang, S. and Z. Du, "A dual-antenna system for LTE/WWAN/WLAN/WiMAX smartphone applications," *IEEE Antennas Wireless Propag. Lett.*, Vol. 14, 1443–1446, 2015.
18. Tang, R. and Z. Du, "Wideband monopole without lumped elements for octa-band narrow-frame LTE smartphone," *IEEE Antennas Wireless Propag. Lett.*, Vol. 16, 720–723, 2017.
19. Yang, Y., Z. Zhao, W. Yang, Z. Nie, and Q.-H. Liu, "Compact multimode monopole antenna for metal-rimmed mobile phones," *IEEE Trans. Antennas Propag.*, Vol. 65, No. 5, 2297–2304, 2017.
20. Liu, Y., P. Liu, Z. Meng, L. Wang, and Y. Li, "A planar printed nona-band loop-monopole reconfigurable antenna for mobile handsets," *IEEE Antennas Wireless Propag. Lett.*, Vol. 17, 1575–1579, 2018.
21. Huang, D., Z. Du, and Y. Wang, "A quad-antenna system for 4G/5G/GPS metal frame mobile phones," *IEEE Antennas Wireless Propag. Lett.*, Vol. 18, 1586–1590, 2019.
22. Tan, Q. and F.-C. Chen, "Triband circularly polarized antenna using a single patch," *IEEE Antennas Wireless Propag. Lett.*, Vol. 19, 2013–2017, 2020.
23. Moreno, R. M., J. Kurvinen, J. Ala-Laurinaho, A. Khripkov, J. Ilvonen, J. van Wonterghem, and V. Viikari, "Dual-polarized mm-wave endfire chain-slot antenna for mobile devices," *IEEE Trans. Antennas Propag.*, Vol. 69, 25–34, 2021.
24. King, R. W. P. and T. T. Wu, "The cylindrical antenna with arbitrary driving point," *IEEE Trans. Antennas Propag.*, Vol. 13, 710–718, 1965.
25. Popovic, B. D., "On polynomial approximation of current along thin asymmetrical cylindrical dipoles," *IEEE Trans. Antennas Propagat.*, Vol. 19, 117–120, 1971.
26. Wang, Y., S. Xu, and D. H. Werner, "1 bit dual-polarized reconfigurable transmitarray antenna using asymmetric dipole elements with parasitic bypass dipoles," *IEEE Trans. Antennas Propag.*, Vol. 69, 1188–1192, 2021.
27. Nesterenko, M. V., V. A. Katrich, Y. M. Penkin, V. M. Dakhov, and S. L. Berdnik, *Thin Impedance Vibrators. Theory and Applications*, Springer Science+Business Media, New York, 2011.
28. Nesterenko, M. V., V. A. Katrich, S. L. Berdnik, Yu. M. Penkin, and V. M. Dakhov, "Application of the generalized method of induced EMF for investigation of characteristics of thin impedance vibrators," *Progress In Electromagnetics Research B*, Vol. 26, 149–178, 2010.
29. Nesterenko, M. V., "Analytical methods in the theory of thin impedance vibrators," *Progress In Electromagnetics Research B*, Vol. 21, 299–328, 2010.
30. King, R. W. P. and G. S. Smith, *Antennas in Matter*, MIT Press, Cambridge, USA 1981.
31. Bretones, R., R. G. Martin, and I. S. García, "Time-domain analysis of magnetic-coated wire antennas," *IEEE Trans. Antennas Propag.*, Vol. 43, 591–596, 1995.
32. Berdnik, S. L., V. A. Katrich, M. V. Nesterenko, Yu. M. Penkin, and D. Yu. Penkin, "Radiation and scattering of electromagnetic waves by a multielement vibrator-slot structure in a rectangular waveguide," *IEEE Trans. Antennas Propag.*, Vol. 63, No. 9, 4256–4259, 2015.
33. Bovkoon, V. P., I. N. Bubnov, A. A. Gridin, and I. N. Zhouk, "Short multifrequency vibrator antenna. II. Engineering calculation of short thick vibrators," *Radio Physics and Radio Astronomy*, Vol. 18, No. 2, 161–168, 2013 (in Russian).
34. Yeliseyeva, N. P., S. L. Berdnik, V. A. Katrich, and M. V. Nesterenko, "Electrodynamic characteristics of horizontal impedance vibrator located over a finite-dimensional perfectly conducting screen," *Progress In Electromagnetics Research B*, Vol. 63, 275–288, 2015.
35. Yeliseyeva, N. P., S. L. Berdnik, V. A. Katrich, and M. V. Nesterenko, "Directional and polarization radiation characteristics of a horizontal impedance vibrator located above a rectangular screen," *Journal of Communications Technology and Electronics*, Vol. 61, No. 2, 99–111, 2016.
36. Yeliseyeva, N. P., V. A. Katrich, M. V. Nesterenko, and S. L. Berdnik, "Characteristics of resonant impedance dipole placed inside dihedral corner reflector," *Proceedings XXIIIth Intern. Seminar on Direct and Inverse Problems of Electromagnetic and Acoustic Wave Theory*, 60–63, 2018.